

CP asymmetries in neutralino production in e^+e^- -collisions

A. BARTL^{a*}, H. FRAAS^{b†}, O. KITTEL^{a,b‡}, W. MAJEROTTO^{c§}

^a *Institut für Theoretische Physik, Universität Wien, Boltzmannngasse 5, A-1090 Wien, Austria*

^b *Institut für Theoretische Physik, Universität Würzburg, Am Hubland, D-97074 Würzburg, Germany*

^c *Institut für Hochenergiephysik, Österreichische Akademie der Wissenschaften, Nikolsdorfgasse 18, A-1050 Wien, Austria*

Abstract

We study two CP sensitive triple-product asymmetries for neutralino production $e^+e^- \rightarrow \tilde{\chi}_i^0 \tilde{\chi}_j^0$ and the subsequent leptonic two-body decay $\tilde{\chi}_i^0 \rightarrow \tilde{\ell} \ell$, $\tilde{\ell} \rightarrow \tilde{\chi}_1^0 \ell$, for $\ell = e, \mu, \tau$. We calculate the asymmetries, cross sections and branching ratios in the Minimal Supersymmetric Standard Model with complex parameters μ and M_1 . We present numerical results for the asymmetries to be expected at a linear electron-positron collider in the 500 GeV range. The asymmetries can go up to 25%. We estimate the event rates which are necessary to observe the asymmetries. Polarized electron and positron beams can significantly enhance the asymmetries and cross sections. In addition, we show how the two decay leptons can be distinguished by making use of their energy distributions.

*e-mail: bartl@ap.univie.ac.at

†e-mail: fraas@physik.uni-wuerzburg.de

‡e-mail: kittel@physik.uni-wuerzburg.de

§e-mail: majer@qhepu3.oeaw.ac.at

1 Introduction

In the Standard Model there is only one physical CP-violating phase in the Cabibbo-Kobayashi-Maskawa matrix. The Minimal Supersymmetric Standard Model (MSSM) [1] contains several new sources of CP violation if the parameters of the model are complex. In the neutralino sector of the MSSM these are the $U(1)$ and $SU(2)$ gaugino mass parameters M_1 and M_2 , respectively, and the higgsino mass parameter μ . One of these parameters, usually M_2 , can be made real by redefining the fields. The non-vanishing phases of M_1 and μ cause CP-violating effects already at tree level, which could be large and thus observable in high energy collider experiments [2].

In this paper we study neutralino production (for recent studies with complex parameters and polarized beams see [3, 4, 5]):

$$e^+ + e^- \rightarrow \tilde{\chi}_i^0 + \tilde{\chi}_j^0 \quad (1)$$

with longitudinally polarized beams and the subsequent leptonic two-body decay of one of the neutralinos

$$\tilde{\chi}_i^0 \rightarrow \tilde{\ell} + \ell_1, \quad (2)$$

and that of the decay slepton

$$\tilde{\ell} \rightarrow \tilde{\chi}_1^0 + \ell_2; \quad \ell = e, \mu, \tau. \quad (3)$$

T-odd observables [3, 6, 7, 8, 9] are a useful tool to study the influence of the CP-violating parameters M_1 and μ . For the neutralino production (1) and the two-body decay chain of the neutralino (2) and (3) we introduce the triple-product

$$\mathcal{T}_I = (\vec{p}_{e^-} \times \vec{p}_{\tilde{\chi}_i}) \cdot \vec{p}_{\ell_1}, \quad (4)$$

and define the corresponding T-odd asymmetry

$$\mathcal{A}_I = \frac{\sigma(\mathcal{T}_I > 0) - \sigma(\mathcal{T}_I < 0)}{\sigma(\mathcal{T}_I > 0) + \sigma(\mathcal{T}_I < 0)}, \quad (5)$$

where σ is the cross section (33) for reactions (1)-(3). Since under time reversal the triple-product changes sign, the asymmetry is a T-odd asymmetry. With the leptonic two-body decay of the slepton Eq. (3), we can construct a further T-odd observable which does not require the identification of the neutralino momentum. We replace the neutralino momentum $\vec{p}_{\tilde{\chi}_i}$ in Eq. (4) by the lepton momentum \vec{p}_{ℓ_2} from the slepton decay, which defines the triple-product:

$$\mathcal{T}_{II} = (\vec{p}_{e^-} \times \vec{p}_{\ell_2}) \cdot \vec{p}_{\ell_1} \quad (6)$$

and the T-odd asymmetry

$$\mathcal{A}_{II} = \frac{\sigma(\mathcal{T}_{II} > 0) - \sigma(\mathcal{T}_{II} < 0)}{\sigma(\mathcal{T}_{II} > 0) + \sigma(\mathcal{T}_{II} < 0)}. \quad (7)$$

Due to CPT invariance these T-odd asymmetries are CP-odd if the widths of the exchanged particles and final state interactions are neglected, which is done in this work.

The T-odd observables in the production of neutralinos at tree level are due to spin effects. Only if there are CP-violating phases in the neutralino sector and if two different neutralinos are produced, each of the produced neutralinos has a polarization vector with a component perpendicular to the production plane [3, 4, 5]. This polarization leads to asymmetries in the angular distributions of the decay products, as defined in Eq. (5) and (7). In general also spin-spin correlations of the neutralinos are present [5]. However, we will not study these in the present work.

In Section 2 we present the formalism used. In Section 3 we discuss the qualitative properties of the asymmetries. We present detailed numerical results in Section 4. Section 5 contains a short summary and conclusion.

2 Definitions and formalism

In this section we give the interaction Lagrangians, the complex couplings and the formulae for the cross section for neutralino production (1) and decay (2),(3). For the definition of the angles for production and decay, see Fig. 1.

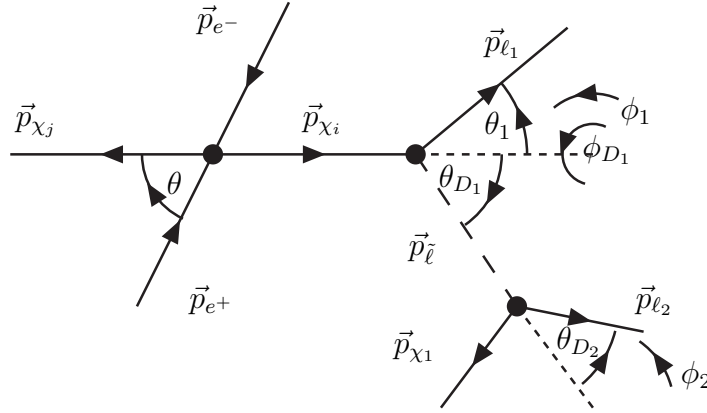


Figure 1: Definition of angles and momenta of the production and decay process.

2.1 Lagrangian and couplings

The interaction Lagrangians for the processes (1)-(3) are (in our notation and conventions we follow closely [1, 5]):

$$\mathcal{L}_{Z^0 \tilde{\chi}_i^0 \tilde{\chi}_j^0} = \frac{1}{2} \frac{g}{\cos \theta_W} Z_\mu \tilde{\chi}_i^0 \gamma^\mu [O_{ij}^{\prime\prime L} P_L + O_{ij}^{\prime\prime R} P_R] \tilde{\chi}_j^0, \quad (8)$$

$$\mathcal{L}_{\ell\tilde{\ell}\tilde{\chi}_i^0} = g f_{\ell i}^L \bar{\ell} P_R \tilde{\chi}_i^0 \tilde{\ell}_L + g f_{\ell i}^R \bar{\ell} P_L \tilde{\chi}_i^0 \tilde{\ell}_R + \text{h.c.}, \quad \ell = e, \mu, \quad i, j = 1, \dots, 4, \quad (9)$$

$$\mathcal{L}_{Z^0\ell^+\ell^-} = -\frac{g}{\cos\theta_W} Z_\mu \bar{\ell} \gamma^\mu [L_\ell P_L + R_\ell P_R] \ell. \quad (10)$$

In the neutralino basis $\tilde{\gamma}, \tilde{Z}, \tilde{H}_a^0, \tilde{H}_b^0$ the couplings are:

$$\begin{aligned} f_{\ell i}^L &= -\sqrt{2} \left[\frac{1}{\cos\theta_W} (T_{3\ell} - e_\ell \sin^2\theta_W) N_{i2} + e_\ell \sin\theta_W N_{i1} \right], \\ f_{\ell i}^R &= -\sqrt{2} e_\ell \sin\theta_W \left[\tan\theta_W N_{i2}^* - N_{i1}^* \right], \end{aligned} \quad (11)$$

$$\begin{aligned} O_{ij}^{\prime\prime L} &= -\frac{1}{2} (N_{i3} N_{j3}^* - N_{i4} N_{j4}^*) \cos 2\beta - \frac{1}{2} (N_{i3} N_{j4}^* + N_{i4} N_{j3}^*) \sin 2\beta, \\ O_{ij}^{\prime\prime R} &= -O_{ij}^{\prime\prime L*}, \text{ with } i, j = 1, \dots, 4. \end{aligned} \quad (12)$$

$$L_\ell = T_{3\ell} - e_\ell \sin^2\theta_W, \quad R_\ell = -e_\ell \sin^2\theta_W. \quad (13)$$

where $P_{L,R} = \frac{1}{2}(1 \mp \gamma_5)$, g is the weak coupling constant ($g = e/\sin\theta_W$, $e > 0$), and e_ℓ and $T_{3\ell}$ denote the charge and the third component of the weak isospin of the lepton ℓ , $\tan\beta = v_2/v_1$ is the ratio of the vacuum expectation values of the two neutral Higgs fields. N_{ij} is the complex unitary 4×4 matrix which diagonalizes the neutral gaugino-higgsino mass matrix $Y_{\alpha\beta}$, $N_{i\alpha}^* Y_{\alpha\beta} N_{\beta k}^\dagger = m_{\tilde{\chi}_i^0} \delta_{ik}$.

For the neutralino decay into staus $\tilde{\chi}_i^0 \rightarrow \tilde{\tau}_k \tau$, we take stau mixing into account and write for the Lagrangian [11]:

$$\mathcal{L}_{\tau\tilde{\tau}\chi_i} = g \tilde{\tau}_k \bar{\tau} (a_{ki}^{\tilde{\tau}} P_R + b_{ki}^{\tilde{\tau}} P_L) \chi_i^0 + \text{h.c.}, \quad k = 1, 2; \quad i = 1, \dots, 4, \quad (14)$$

with

$$a_{kj}^{\tilde{\tau}} = (\mathcal{R}_{kn}^{\tilde{\tau}})^* \mathcal{A}_{jn}^\tau, \quad b_{kj}^{\tilde{\tau}} = (\mathcal{R}_{kn}^{\tilde{\tau}})^* \mathcal{B}_{jn}^\tau, \quad (n = L, R) \quad (15)$$

$$\mathcal{A}_j^\tau = \begin{pmatrix} f_{\tau j}^L \\ h_{\tau j}^R \end{pmatrix}, \quad \mathcal{B}_j^\tau = \begin{pmatrix} h_{\tau j}^L \\ f_{\tau j}^R \end{pmatrix}, \quad (16)$$

with $\mathcal{R}_{kn}^{\tilde{\tau}}$ the stau mixing matrix defined below and

$$h_{\tau j}^L = (h_{\tau j}^R)^* = -Y_\tau (N_{j3}^* \cos\beta + N_{j4}^* \sin\beta), \quad (17)$$

$$Y_\tau = m_\tau / (\sqrt{2} m_W \cos\beta), \quad (18)$$

with m_W the mass of the W boson and m_τ the mass of the τ -lepton. The masses and couplings of the τ -sleptons follow from the hermitian 2×2 $\tilde{\tau}_L - \tilde{\tau}_R$ mixing matrix:

$$\mathcal{L}_M^{\tilde{\tau}} = -(\tilde{\tau}_L^*, \tilde{\tau}_R^*) \begin{pmatrix} M_{\tilde{\tau}_{LL}}^2 & e^{-i\varphi_{\tilde{\tau}}} |M_{\tilde{\tau}_{LR}}^2| \\ e^{i\varphi_{\tilde{\tau}}} |M_{\tilde{\tau}_{LR}}^2| & M_{\tilde{\tau}_{RR}}^2 \end{pmatrix} \begin{pmatrix} \tilde{\tau}_L \\ \tilde{\tau}_R \end{pmatrix}, \quad (19)$$

with

$$M_{\tilde{\tau}_{LL}}^2 = m_{\tilde{\ell}_L}^2 + m_\tau^2, \quad (20)$$

$$M_{\tilde{\tau}_{RR}}^2 = m_{\tilde{\ell}_R}^2 + m_\tau^2, \quad (21)$$

$$M_{\tilde{\tau}_{RL}}^2 = (M_{\tilde{\tau}_{LR}}^2)^* = m_\tau(A_\tau - \mu^* \tan \beta), \quad (22)$$

$$\varphi_{\tilde{\tau}} = \arg[A_\tau - \mu^* \tan \beta], \quad (23)$$

A_τ is the complex trilinear scalar coupling parameter. The $\tilde{\tau}$ mass eigenstates are $(\tilde{\tau}_1, \tilde{\tau}_2) = (\tilde{\tau}_L, \tilde{\tau}_R)\mathcal{R}^{\tilde{\tau}T}$ with

$$\mathcal{R}^{\tilde{\tau}} = \begin{pmatrix} e^{i\varphi_{\tilde{\tau}}} \cos \theta_{\tilde{\tau}} & \sin \theta_{\tilde{\tau}} \\ -\sin \theta_{\tilde{\tau}} & e^{-i\varphi_{\tilde{\tau}}} \cos \theta_{\tilde{\tau}} \end{pmatrix}, \quad (24)$$

and

$$\cos \theta_{\tilde{\tau}} = \frac{-|M_{\tilde{\tau}_{LR}}^2|}{\sqrt{|M_{\tilde{\tau}_{LR}}^2|^2 + (m_{\tilde{\tau}_1}^2 - M_{\tilde{\tau}_{LL}}^2)^2}}, \quad \sin \theta_{\tilde{\tau}} = \frac{M_{\tilde{\tau}_{LL}}^2 - m_{\tilde{\tau}_1}^2}{\sqrt{|M_{\tilde{\tau}_{LR}}^2|^2 + (m_{\tilde{\tau}_1}^2 - M_{\tilde{\tau}_{LL}}^2)^2}}. \quad (25)$$

The mass eigenvalues are

$$m_{\tilde{\tau}_{1,2}}^2 = \frac{1}{2} \left((M_{\tilde{\tau}_{LL}}^2 + M_{\tilde{\tau}_{RR}}^2) \mp \sqrt{(M_{\tilde{\tau}_{LL}}^2 - M_{\tilde{\tau}_{RR}}^2)^2 + 4|M_{\tilde{\tau}_{LR}}^2|^2} \right). \quad (26)$$

In order to reduce the number of MSSM parameters, we assume the renormalization group equations (RGE) for the slepton masses [12]:

$$m_{\tilde{\ell}_R}^2 = m_0^2 + 0.23M_2^2 - m_Z^2 \cos 2\beta \sin^2 \theta_W, \quad (27)$$

$$m_{\tilde{\ell}_L}^2 = m_0^2 + 0.79M_2^2 + m_Z^2 \cos 2\beta \left(-\frac{1}{2} + \sin^2 \theta_W\right), \quad (28)$$

where m_Z is the mass of the Z boson and m_0 is the scalar mass parameter.

2.2 Cross sections

In order to calculate the amplitude squared for the complete process of neutralino production (1) and the two-body decay chain of the neutralino $\tilde{\chi}_i^0$ (2)-(3), we use the spin density matrix formalism of [5, 10]. The amplitude squared can be written as:

$$|T|^2 = 2 \sum_{\lambda_i \lambda'_i} |\Delta(\tilde{\chi}_i^0)|^2 |\Delta(\tilde{\ell})|^2 \rho_P(\tilde{\chi}_i^0)^{\lambda_i \lambda'_i} \rho_{D1}(\tilde{\chi}_i^0)_{\lambda'_i \lambda_i} D_2(\tilde{\ell}), \quad (29)$$

with $\rho_P(\tilde{\chi}_i^0)$ the spin density production matrix of neutralino $\tilde{\chi}_i^0$, the propagator $\Delta(\tilde{\chi}_i^0) = 1/[s_{\chi_i} - m_{\chi_i}^2 + im_{\chi_i}\Gamma_{\chi_i}]$, the decay matrix $\rho_{D1}(\tilde{\chi}_i^0)$ for decay (2), the slepton propagator $\Delta(\tilde{\ell}) = 1/[s_{\tilde{\ell}} - m_{\tilde{\ell}}^2 + im_{\tilde{\ell}}\Gamma_{\tilde{\ell}}]$, and the factor $D_2(\tilde{\ell})$ for the slepton decay (3). In Eq. (29), λ_i

and λ'_i are the helicities of the neutralino $\tilde{\chi}_i^0$ and $s_{\chi_i} = p_{\chi_i}^2 (s_{\tilde{\ell}} = p_{\tilde{\ell}}^2)$, the mass and width of $\tilde{\chi}_i^0$ ($\tilde{\ell}$) are denoted by m_{χ_i} ($m_{\tilde{\ell}}$) and Γ_{χ_i} ($\Gamma_{\tilde{\ell}}$), respectively. The factor 2 is due to the summation of the helicities of the second neutralino $\tilde{\chi}_j^0$, whose decay is not considered.

The spin basis vectors $s_{\chi_i}^a$ ($a = 1, 2, 3$) of the neutralino $\tilde{\chi}_i^0$ fulfill the orthonormality relations $s_{\chi_i}^a \cdot s_{\chi_i}^b = -\delta^{ab}$ and $s_{\chi_i}^a \cdot p_{\chi_i} = 0$. Their explicit form is given in Appendix A. The (unnormalized) density matrices can then be expanded in terms of the Pauli matrices:

$$\rho_P(\tilde{\chi}_i^0)^{\lambda_i \lambda'_i} = \delta_{\lambda_i \lambda'_i} P + \sum_a \sigma_{\lambda_i \lambda'_i}^a \Sigma_P^a, \quad (30)$$

$$\rho_{D1}(\tilde{\chi}_i^0)^{\lambda'_i \lambda_i} = \delta_{\lambda'_i \lambda_i} D_1 + \sum_a \sigma_{\lambda'_i \lambda_i}^a \Sigma_{D1}^a. \quad (31)$$

With our choice of the spin vectors, $\frac{\Sigma_P^3}{P}$ is the longitudinal polarization of neutralino $\tilde{\chi}_i^0$, $\frac{\Sigma_P^1}{P}$ is the transverse polarization in the production plane and $\frac{\Sigma_P^2}{P}$ is the polarization perpendicular to the production plane. The analytical formulae for P , D_1 , D_2 and Σ_P^2 , Σ_{D1}^a are given in Appendix C. Inserting the density matrices (30) and (31) in Eq. (29) leads to:

$$|T|^2 = 4 |\Delta(\tilde{\chi}_i^0)|^2 |\Delta(\tilde{\ell})|^2 (P D_1 + \vec{\Sigma}_P \vec{\Sigma}_{D1}) D_2. \quad (32)$$

The cross section and distributions in the laboratory system are then obtained by integrating $|T|^2$ over the Lorentz invariant phase space element $d\text{Lips}(s, p_{\chi_j}, p_{\ell_1}, p_{\chi_1}, p_{\ell_2})$ (B.1):

$$d\sigma = \frac{1}{2s} |T|^2 d\text{Lips}(s, p_{\chi_j}, p_{\ell_1}, p_{\chi_1}, p_{\ell_2}), \quad (33)$$

where we use the narrow width approximation for the propagators.

The contributions of the spin correlation terms $\vec{\Sigma}_P \vec{\Sigma}_{D1}$ to the total cross section vanish. Their contributions to the energy distributions of the lepton ℓ_1 and ℓ_2 from decay (2) and (3) vanish due to the Majorana properties of the neutralinos [13] if CP is conserved. If CP is violated, they vanish to leading order perturbation theory [13]. In our case, the contributions can be neglected because they are proportional to the widths of the exchanged particles.

3 T-odd asymmetry

The asymmetry \mathcal{A}_I , defined in Eq. (5), can be written in terms of the angular distribution of the decay lepton ℓ_1 :

$$\mathcal{A}_I = \frac{\int_1^0 \frac{d\sigma}{d\cos\theta_I} d\cos\theta_I - \int_0^{-1} \frac{d\sigma}{d\cos\theta_I} d\cos\theta_I}{\int_1^0 \frac{d\sigma}{d\cos\theta_I} d\cos\theta_I + \int_0^{-1} \frac{d\sigma}{d\cos\theta_I} d\cos\theta_I} = \frac{N_+ - N_-}{N_+ + N_-}, \quad (34)$$

where $\cos\theta_I = \frac{\vec{p}_{e^-} \times \vec{p}_{\chi_i}}{|\vec{p}_{e^-} \times \vec{p}_{\chi_i}|} \cdot \frac{\vec{p}_{\ell_1}}{|\vec{p}_{\ell_1}|}$ and thus \mathcal{A}_I is the difference of the number of events with lepton ℓ_1 above (N_+) and below (N_-) the production plane, normalized by the total

number of events. In order to measure the asymmetry \mathcal{A}_I , the production plane and thus the momentum \vec{p}_{χ_i} of neutralino $\tilde{\chi}_i^0$ has to be reconstructed. We will discuss in Section 4.4 how to distinguish the two leptons.

Analogously the asymmetry \mathcal{A}_{II} , defined in Eq. (7), can be written in terms of the angular distribution of the decay leptons ℓ_1 and ℓ_2 :

$$\mathcal{A}_{II} = \frac{\int_1^0 \frac{d\sigma}{d\cos\theta_{II}} d\cos\theta_{II} - \int_0^{-1} \frac{d\sigma}{d\cos\theta_{II}} d\cos\theta_{II}}{\int_1^0 \frac{d\sigma}{d\cos\theta_{II}} d\cos\theta_{II} + \int_0^{-1} \frac{d\sigma}{d\cos\theta_{II}} d\cos\theta_{II}}, \quad (35)$$

where $\cos\theta_{II} = \frac{\vec{p}_{e^-} \times \vec{p}_{\ell_2}}{|\vec{p}_{e^-} \times \vec{p}_{\ell_2}|} \cdot \frac{\vec{p}_{\ell_1}}{|\vec{p}_{\ell_1}|}$. Inserting the cross section (33) in the definitions of the asymmetries (5) and (7) we obtain:

$$\mathcal{A}_{I,II} = \frac{\int \text{Sign}[\mathcal{T}_{I,II}] |T|^2 d\text{Lips}}{\int |T|^2 d\text{Lips}} = \frac{\int \text{Sign}[\mathcal{T}_{I,II}] \Sigma_P^2 \Sigma_{D1}^2 d\text{Lips}}{\int P D_1 d\text{Lips}}, \quad (36)$$

with $d\text{Lips} = d\text{Lips}(s, p_{\chi_i}, p_{\chi_j}) d\text{Lips}(s_{\chi_i}, p_{\tilde{\ell}}, p_{\ell_1}) d\text{Lips}(s_{\tilde{\ell}}, p_{\chi_1}, p_{\ell_2}) \delta(s_{\chi_i} - m_{\chi_i}^2) \delta(s_{\tilde{\ell}} - m_{\tilde{\ell}}^2)$, see Eq. (B.1). In the numerator only the spin correlation terms perpendicular to the production plane $\Sigma_P^2 \Sigma_{D1}^2$ remain, since only Σ_P^2 contains the triple-products (4) or (6). Thus, the contributions to $\mathcal{A}_{I,II}$ directly stem from Σ_P^2 .

In case the neutralino decays into a scalar tau, we take stau mixing into account and the asymmetries are reduced due to their qualitative dependence on the $\tilde{\chi}_i^0$ - $\tilde{\tau}_k$ - τ couplings:

$$\mathcal{A}_{I,II} \propto \frac{|a_{ki}^{\tilde{\tau}}|^2 - |b_{ki}^{\tilde{\tau}}|^2}{|a_{ki}^{\tilde{\tau}}|^2 + |b_{ki}^{\tilde{\tau}}|^2}, \quad (37)$$

which can be seen from the expressions of D_1 (C.15) and Σ_{D1}^2 (C.16). Because the asymmetry is only proportional to the absolute values of $a_{ki}^{\tilde{\tau}}, b_{ki}^{\tilde{\tau}}$, it is not sensitive to a possible phase φ_{A_τ} of A_τ . In order to be sensitive to φ_{A_τ} , one would have to consider an asymmetry which involves the transverse polarization of the τ .

4 Numerical results

In the following numerical analysis we study for $\sqrt{s} = 500$ and longitudinally polarized beams with $P_- = 0.8$ and $P_+ = -0.6$, the dependence of the neutralino production cross sections $\sigma(e^+e^- \rightarrow \tilde{\chi}_i^0 \tilde{\chi}_j^0)$, the branching ratios $BR(\tilde{\chi}_i^0 \rightarrow \tilde{\ell} \ell)$ and the asymmetries \mathcal{A}_I and \mathcal{A}_{II} on the parameters $\mu = |\mu| e^{i\varphi_\mu}$, $M_1 = |M_1| e^{i\varphi_{M1}}$ and M_2 for $\tan\beta = 10$. In order to reduce the number of parameters, we assume $|M_1| = 5/3 \tan^2\theta_W M_2$ and in Eqs. (27) and (28) we take $m_0 = 100$ GeV for the slepton masses. Since the pair production of equal neutralinos is not CP sensitive, we discuss the lightest unequal pairs $\tilde{\chi}_1^0 \tilde{\chi}_2^0$, $\tilde{\chi}_1^0 \tilde{\chi}_3^0$ and $\tilde{\chi}_2^0 \tilde{\chi}_3^0$.

4.1 Production of $\tilde{\chi}_1^0 \tilde{\chi}_2^0$

In Fig. 2a we show the cross section for $\tilde{\chi}_1^0 \tilde{\chi}_2^0$ production for $\varphi_\mu = 0$ and $\varphi_{M_1} = 0.5 \pi$ in the $|\mu|-M_2$ plane. The cross section reaches values up to 300 fb. For $|\mu| \lesssim 250$ GeV the right selectron exchange dominates so that our choice of polarization $P_- = 0.8$ and $P_+ = -0.6$ enhances the cross section by a factor as large as 2.5 compared to the unpolarized case. For $|\mu| \gtrsim 300$ GeV the left selectron exchange dominates because of the larger $\tilde{\chi}_2^0 - \tilde{e}_L$ coupling. In this region a sign reversal of both polarizations would enhance the cross section by a factor between 1 and 20.

The branching ratio for the neutralino two-body decay into right selectrons and smuons $\text{BR}(\tilde{\chi}_2^0 \rightarrow \tilde{\ell}_R \ell_1)$ (summed over both signs of charge) is shown in Fig. 2b. The branching ratio reaches values up to 64% and decreases with increasing $|\mu|$ when the two-body decays into the lightest neutral Higgs boson h^0 and/or the Z boson are kinematically allowed. The channels into the W boson do not open. With our choice for the slepton masses, Eqs. (27) and (28), the decay into left selectrons and smuons can be neglected because these channels are either not open or the branching fraction is smaller than 1%. As we assume that the squarks and the other Higgs bosons are heavy, the decay into the stau is a competing channel, which is discussed below. In our scenario this decay mode dominates for $M_2 \lesssim 200$ GeV, see Fig. 4a. The resulting cross section $\sigma(e^+e^- \rightarrow \tilde{\chi}_1^0 \tilde{\chi}_2^0) \times \text{BR}(\tilde{\chi}_2^0 \rightarrow \tilde{\ell}_R \ell_1) \times \text{BR}(\tilde{\ell}_R \rightarrow \tilde{\chi}_1^0 \ell_2)$ with $\text{BR}(\tilde{\ell}_R \rightarrow \tilde{\chi}_1^0 \ell_2) = 1$ is shown in Fig. 2c.

Fig. 2d shows the $|\mu|-M_2$ dependence of the asymmetry \mathcal{A}_{II} for $\varphi_{M_1} = 0.5 \pi$ and $\varphi_\mu = 0$. In the region $|\mu| \lesssim 250$ GeV, where the right selectron exchange dominates, the asymmetry reaches 9.5% for our choice of beam polarization. This enhances the asymmetry up to a factor of 2 compared to the case of unpolarized beams. With increasing $|\mu|$ the asymmetry decreases and finally changes sign. This is due to the increasing contributions of the left selectron exchange which contributes to the asymmetry with opposite sign and dominates for $|\mu| \gtrsim 300$ GeV. In this region the asymmetry could be enhanced up to a factor 2 by reversing the sign of both beam polarizations.

The sensitivity of the cross section σ and the asymmetry \mathcal{A}_{II} on the CP phases can be seen by contour plots in the $\varphi_\mu-\varphi_{M_1}$ plane, for $|\mu| = 240$ GeV and $M_2 = 400$ GeV (Fig. 3). In our scenario the variation of the cross section (Fig. 3a) is more than 100%. In addition to the CP sensitive observables, the cross section may also serve to determine the values of the phases. Using unpolarized beams, the cross section would be reduced by a factor 0.4. The asymmetry \mathcal{A}_{II} (Fig. 3b) varies between -8.9% and 8.9%. It is remarkable that these maximal values are not necessarily obtained for maximal CP phases. In our scenario the asymmetry is much more sensitive to variations of the phase φ_{M_1} around 0. On the other hand, the asymmetry is rather insensitive to φ_μ . For unpolarized beams this asymmetry would be reduced roughly by a factor 0.33.

The relative statistical error of each asymmetry \mathcal{A} can be calculated to $\delta\mathcal{A} = \Delta\mathcal{A}/\mathcal{A} = S/(\mathcal{A}\sqrt{N})$, with S standard deviations, assuming a Gaussian distribution of the asymmetry \mathcal{A} . Here, $N = \mathcal{L}\sigma$ is the number of events with \mathcal{L} the total integrated luminosity and σ the total cross section. Assuming $\delta\mathcal{A} \approx 1$, it follows $S \approx \mathcal{A}\sqrt{N}$. For example, in order to measure an asymmetry of 5% with $S=2$ (confidence level of 95%), one would need at

least 1.5×10^3 events. This corresponds to a total cross section for reactions (1)-(3) of 3.1 fb with $\mathcal{L} = 500 \text{ fb}^{-1}$. We show the contour lines of $S = 3$ and 5 for \mathcal{A}_{II} in Fig. 3c with $\mathcal{L} = 500 \text{ fb}^{-1}$. In the gray shaded area $S < 3$.

In Fig. 3d we also show the asymmetry \mathcal{A}_I which is a factor 2.9 larger than \mathcal{A}_{II} , because in \mathcal{A}_{II} the CP-violating effect from the production is washed out by the kinematics of the slepton decay. However, for a measurement of \mathcal{A}_I the reconstruction of the $\tilde{\chi}_2^0$ momentum is necessary. The asymmetry \mathcal{A}_I shows a similar dependence on the phases as \mathcal{A}_{II} because both are due to the non vanishing neutralino polarization perpendicular to the production plane.

It is interesting to note that, due to the weak dependence on φ_μ , the asymmetries can be sizable for $\varphi_\mu \approx 0$. Small values for φ_μ are suggested by constraints on electron and neutron electric dipole moments (EDMs) [14] for a typical SUSY scale of the order of a few 100 GeV (for a review see, e.g., [15]).

Next we want to comment on the neutralino decay into the scalar tau and discuss the main differences from the decay into the selectron and smuon. In some regions of the parameter space, the decay of the neutralino into the lightest stau $\tilde{\tau}_1$ may dominate over that into the right selectron and smuon, and may even be the only decay channel. In Fig. 4a we show the branching ratio $BR(\tilde{\chi}_2^0 \rightarrow \tilde{\tau}_1 \tau)$ in the $|\mu|$ - M_2 plane for $A_\tau = -250$ GeV, $\varphi_{M_1} = 0.5\pi$ and $\varphi_\mu = 0$. For $M_2 < 200$ GeV the branching ratio $BR(\tilde{\chi}_2^0 \rightarrow \tilde{\tau}_1 \tau)$ is larger than 80%. However, due to the mixing in the stau sector the asymmetry \mathcal{A}_{II} , Fig. 4b, is reduced compared to that in the selectron and smuon channels, see Fig. 2d. The reason is the suppression factor $(|a_{\tilde{\tau}ki}|^2 - |b_{\tilde{\tau}ki}|^2)/(|a_{\tilde{\tau}ki}|^2 + |b_{\tilde{\tau}ki}|^2)$, Eq. (37), which may be small or even be zero. This may lead to a reduced or vanishing asymmetry, respectively, even in the case of non zero CP phases.

4.2 Production of $\tilde{\chi}_1^0 \tilde{\chi}_3^0$

We show in Fig. 5a and b contour plots of the cross section $\sigma(e^+e^- \rightarrow \tilde{\chi}_1^0 \tilde{\chi}_3^0) \times BR(\tilde{\chi}_3^0 \rightarrow \tilde{\ell}_R \ell_1) \times BR(\tilde{\ell}_R \rightarrow \tilde{\chi}_1^0 \ell_2)$ with $BR(\tilde{\ell}_R \rightarrow \tilde{\chi}_1^0 \ell_2) = 1$ and of the asymmetry \mathcal{A}_{II} , respectively. The cross section with polarized beams reaches more than 100 fb, which is up to a factor 2.5 larger than for unpolarized beams. The asymmetry \mathcal{A}_{II} , shown in Fig. 5b, reaches -9.5%. For unpolarized beams this value would be reduced by a factor 0.75. For our choice of parameters the cross section and the asymmetry for $\tilde{\chi}_1^0 \tilde{\chi}_3^0$ production and decay show a similar dependence on M_2 and $|\mu|$ as for $\tilde{\chi}_1^0 \tilde{\chi}_2^0$ production, however, the kinematically allowed regions are different. We also studied the φ_μ dependence of \mathcal{A}_{II} . For $\varphi_\mu = 0.5\pi(0.1\pi)$ and $\varphi_{M_1} = 0$, the maximal values of \mathcal{A}_{II} in the M_2 - $|\mu|$ plane are $|\mathcal{A}_{II}| < 3\%(1\%)$.

4.3 Production of $\tilde{\chi}_2^0 \tilde{\chi}_3^0$

The production of the neutralino pair $e^+e^- \rightarrow \tilde{\chi}_2^0 \tilde{\chi}_3^0$ could make it easier to reconstruct the production plane because both neutralinos decay. This allows one to determine also asymmetry \mathcal{A}_I , which is a factor 2-3 larger than \mathcal{A}_{II} . We discuss the decay of the heavier

neutralino $\tilde{\chi}_3^0$, which has a larger kinematically allowed region in the $|\mu|-M_2$ plane than that of $\tilde{\chi}_2^0$. In Fig. 6 we display the production cross section $\sigma(e^+e^- \rightarrow \tilde{\chi}_2^0\tilde{\chi}_3^0)$ which reaches 100 fb. The cross section $\sigma(e^+e^- \rightarrow \tilde{\chi}_2^0\tilde{\chi}_3^0) \times BR(\tilde{\chi}_3^0 \rightarrow \tilde{\ell}_R\ell_1) \times BR(\ell_R \rightarrow \tilde{\chi}_1^0\ell_2)$ with $BR(\tilde{\ell}_R \rightarrow \tilde{\chi}_1^0\ell_2) = 1$ is shown in Fig. 6b. The asymmetry \mathcal{A}_{II} is shown in Fig. 6d. As to the φ_μ dependence of \mathcal{A}_I , we found that for $\varphi_\mu = 0.5\pi(0.1\pi)$ and $\varphi_{M_1} = 0$, $|\mathcal{A}_I|$ can reach 25% (2%) in the $M_2-|\mu|$ plane.

4.4 Energy distributions of the leptons

In order to measure the asymmetries \mathcal{A}_I (5) and \mathcal{A}_{II} (7), the two leptons ℓ_1 and ℓ_2 from the neutralino (2) and slepton decay (3) have to be distinguished. We therefore calculate the energy distributions of the leptons from the first and second decay vertex in the laboratory system (i.e. the cms of the incoming e^+ and e^- beams). One can distinguish between the two leptons event by event, if their energy distributions do not overlap. If their energy distributions do overlap, only those leptons can be distinguished, whose energies are not both in the overlapping region.

The energy distribution of lepton ℓ_1 in the laboratory system has the form of a box with the endpoints:

$$E_{\ell_1, \min, \max} = \frac{m_{\chi_i}^2 - m_{\tilde{\ell}}^2}{2(E_{\chi_i} \pm q)}, \quad (38)$$

with q the neutralino momentum. The energy distribution of the second lepton ℓ_2 is obtained by integrating over the energy $E_{\tilde{\ell}}$ of the propagating slepton:

$$\frac{1}{\sigma} \frac{d\sigma}{dE_{\ell_2}} = \frac{m_{\tilde{\ell}}^2 m_{\chi_i}^2}{q[m_{\chi_i}^2 - m_{\tilde{\ell}}^2][m_{\tilde{\ell}}^2 - m_{\chi_1}^2]} \times \begin{cases} \ln \frac{E_{\ell_2}}{A} & ; \quad A \leq E_{\ell_2} \leq a \\ \ln \frac{a}{A} & ; \quad a \leq E_{\ell_2} \leq b \\ \ln \frac{B}{E_{\ell_2}} & ; \quad b \leq E_{\ell_2} \leq B \end{cases} \quad (39)$$

with:

$$A, B = \frac{m_{\tilde{\ell}}^2 - m_{\chi_1}^2}{2m_{\tilde{\ell}}^2} \left(E_{\tilde{\ell}, \max} \mp \sqrt{E_{\tilde{\ell}, \max}^2 - m_{\tilde{\ell}}^2} \right) \quad (40)$$

$$a, b = \frac{m_{\tilde{\ell}}^2 - m_{\chi_1}^2}{2m_{\tilde{\ell}}^2} \left(E_{\tilde{\ell}, \min} \mp \sqrt{E_{\tilde{\ell}, \min}^2 - m_{\tilde{\ell}}^2} \right) \quad (41)$$

$$E_{\tilde{\ell}, \max, \min} = \frac{E_{\chi_i}(m_{\chi_i}^2 + m_{\tilde{\ell}}^2) \pm (m_{\chi_i}^2 - m_{\tilde{\ell}}^2)\sqrt{E_{\chi_i}^2 - m_{\chi_i}^2}}{2m_{\chi_i}^2}. \quad (42)$$

We show in Figs. 7a - c an example of the energy distributions of lepton ℓ_1 (dashed line), and lepton ℓ_2 (solid line), $\ell = e, \mu$, for $e^+e^- \rightarrow \tilde{\chi}_1^0\tilde{\chi}_2^0$ and the subsequent decays $\tilde{\chi}_2^0 \rightarrow \tilde{\ell}\ell_1$ and $\tilde{\ell} \rightarrow \tilde{\chi}_1^0\ell_2$, for $\tan\beta = 10$, $M_2 = 300$ GeV, $\varphi_\mu = 0$ and $\varphi_{M_1} = 0.5\pi$ for $|\mu| = 200, 300$ and 500 GeV, respectively. The parameters are chosen such that the slepton mass $m_{\tilde{\ell}_R} = 180$ GeV is constant, the LSP mass $m_{\chi_1} = 140, 145, 150$ GeV

is almost constant whereas the neutralino mass $m_{\tilde{\chi}_2} = 185, 240, 300$ GeV is increasing. The mass difference between $\tilde{\ell}_R$ and $\tilde{\chi}_1^0$ decreases ($\Delta m = 40, 35, 30$ GeV), whereas the mass difference between $\tilde{\chi}_2^0$ and $\tilde{\ell}_R$ increases ($\Delta m = 5, 60, 120$ GeV). The endpoints of the energy distributions of the decay leptons depend on these mass differences. Thus, in Fig. 7a, the second lepton is more energetic than the first lepton. The energy distributions do not overlap and thus the two leptons can be distinguished by measuring their energies. This also holds for Fig. 7c, where the first lepton is more energetic than the second one. In Fig. 7b the two distributions overlap because the mass differences between $\tilde{\chi}_1^0$, $\tilde{\ell}_R$ and $\tilde{\chi}_2^0$ are similar. One has to apply cuts in order to distinguish the two leptons, which reduce the number of events.

A potentially large background may be due to slepton production $e^+e^- \rightarrow \tilde{\ell}^+\tilde{\ell}^- \rightarrow \ell^+\ell^-\tilde{\chi}_1^0\tilde{\chi}_1^0$. However, these reactions would lead generally to "two-sided events", whereas the events from $e^+e^- \rightarrow \tilde{\chi}_1^0\tilde{\chi}_i^0 \rightarrow \ell^+\ell^-\tilde{\chi}_1^0\tilde{\chi}_1^0$ are "one-sided events". Moreover, the background reaction is CP-even and will not give rise to a CP asymmetry, because the sleptons are scalars and their decay is a two-body one.

5 Summary and conclusion

We have considered two CP sensitive triple-product asymmetries in neutralino production $e^+e^- \rightarrow \tilde{\chi}_i^0\tilde{\chi}_j^0$ and the subsequent leptonic two-body decay chain of one neutralino $\tilde{\chi}_i^0 \rightarrow \tilde{\ell}\ell$, $\tilde{\ell} \rightarrow \tilde{\chi}_1^0\ell$ for $\ell = e, \mu, \tau$. The CP sensitive contributions to the asymmetries are present already at tree level and are due to spin effects in the production process of two different neutralinos. The asymmetries are induced only if CP-violating phases of the gaugino and higgsino mass parameters M_1 and/or μ are present in the neutralino sector of the MSSM.

In a numerical study for $e^+e^- \rightarrow \tilde{\chi}_1^0\tilde{\chi}_2^0$ and neutralino decay into a right slepton $\tilde{\chi}_2^0 \rightarrow \tilde{\ell}_R\ell$ we have shown that the asymmetries can be as large as 25%. They can be sizeable even for a small phase of μ , which is suggested by the experimental limits on EDMs. The asymmetries are similar for the processes $e^+e^- \rightarrow \tilde{\chi}_1^0\tilde{\chi}_3^0$ and $e^+e^- \rightarrow \tilde{\chi}_2^0\tilde{\chi}_3^0$. Depending on the MSSM scenario, our proposed asymmetries should be accessible in future electron-positron linear collider experiments in the 500 GeV range. Longitudinally polarized electron and positron beams can considerably enhance both asymmetries and production cross sections.

6 Acknowledgement

We thank S. Hesselbach and T. Kernreiter for useful discussions. This work was supported by the 'Fonds zur Förderung der wissenschaftlichen Forschung' (FWF) of Austria, projects No. P13139-PHY and No. P16592-N02 and by the European Community's Human Potential Programme under contract HPRN-CT-2000-00149. This work was also supported by the 'Deutsche Forschungsgemeinschaft' (DFG) under contract Fr 1064/5-1. O.K. acknowledges support from the *Bayerische Julius-Maximilians Universität Würzburg*.

Appendix

A Momentum and spin vectors

We choose a coordinate frame in the center of mass system such that the momentum of neutralino $\tilde{\chi}_j^0$ points in the z -direction. The scattering angle is $\theta \angle(\vec{p}_{e^-}, \vec{p}_{\tilde{\chi}_j})$ and the azimuth ϕ can be chosen to zero. The momenta are given by:

$$p_{e^-} = E_b(1, -\sin \theta, 0, \cos \theta), \quad p_{e^+} = E_b(1, \sin \theta, 0, -\cos \theta), \quad (\text{A.1})$$

$$p_{\chi_i} = (E_{\chi_i}, 0, 0, -q), \quad p_{\chi_j} = (E_{\chi_j}, 0, 0, q), \quad (\text{A.2})$$

with the beam energy $E_b = \sqrt{s}/2$ and

$$E_{\chi_i} = \frac{s + m_{\chi_i}^2 - m_{\chi_j}^2}{2\sqrt{s}}, \quad E_{\chi_j} = \frac{s + m_{\chi_j}^2 - m_{\chi_i}^2}{2\sqrt{s}}, \quad q = \frac{\lambda^{\frac{1}{2}}(s, m_{\chi_i}^2, m_{\chi_j}^2)}{2\sqrt{s}}, \quad (\text{A.3})$$

with m_{χ_i}, m_{χ_j} the masses of the neutralinos and $\lambda(x, y, z) = x^2 + y^2 + z^2 - 2xy - 2xz - 2yz$. The three spin basis vectors of $\tilde{\chi}_i^0$ are chosen by:

$$s_{\chi_i}^1 = (0, -1, 0, 0), \quad s_{\chi_i}^2 = (0, 0, 1, 0), \quad s_{\chi_i}^3 = \frac{1}{m_{\chi_i}}(q, 0, 0, -E_{\chi_i}). \quad (\text{A.4})$$

Together with the unit momentum vector p_{χ_i}/m_{χ_i} of $\tilde{\chi}_i^0$, the spin basis vectors form an orthonormal set. The momenta and energies of the leptons are:

$$p_{\ell_1} = (E_{\ell_1}, -|\vec{p}_{\ell_1}| \sin \theta_1 \cos \phi_1, |\vec{p}_{\ell_1}| \sin \theta_1 \sin \phi_1, -|\vec{p}_{\ell_1}| \cos \theta_1), \quad (\text{A.5})$$

$$p_{\ell_2} = (E_{\ell_2}, -|\vec{p}_{\ell_2}| \sin \theta_2 \cos \phi_2, |\vec{p}_{\ell_2}| \sin \theta_2 \sin \phi_2, -|\vec{p}_{\ell_2}| \cos \theta_2), \quad (\text{A.6})$$

$$E_{\ell_1} = |\vec{p}_{\ell_1}| = \frac{m_{\chi_i}^2 - m_{\tilde{\ell}}^2}{2(E_{\chi_i} - q \cos \theta_1)}, \quad E_{\ell_2} = |\vec{p}_{\ell_2}| = \frac{m_{\tilde{\ell}}^2 - m_{\chi_1}^2}{2(E_{\tilde{\ell}} - |\vec{p}_{\chi_i} - \vec{p}_{\ell_1}| \cos \theta_{D_2})}, \quad (\text{A.7})$$

with $\theta_1 = \angle(\vec{p}_{\ell_1}, \vec{p}_{\chi_i})$, $\theta_2 = \angle(\vec{p}_{\ell_2}, \vec{p}_{\chi_i})$ and the decay angles $\theta_{D_2} \angle(\vec{p}_{\tilde{\ell}}, \vec{p}_{\ell_2})$ and $\theta_{D_1} \angle(\vec{p}_{\chi_i}, \vec{p}_{\tilde{\ell}})$ (see Fig. 1):

$$\cos \theta_{D_2} = \cos \theta_{D_1} \cos \theta_2 - \sin \theta_{D_1} \sin \theta_2 \cos(\phi_2 - \phi_1), \quad \cos \theta_{D_1} = \frac{\vec{p}_{\chi_i}(\vec{p}_{\chi_i} - \vec{p}_{\ell_1})}{|\vec{p}_{\chi_i}| |\vec{p}_{\chi_i} - \vec{p}_{\ell_1}|}. \quad (\text{A.8})$$

B Phase space

The Lorentz invariant phase space element for the neutralino production (1) and the decay chain (2)-(3) can be decomposed into the two-body phase space elements:

$$d\text{Lips}(s, p_{\chi_j}, p_{\ell_1}, p_{\chi_1}, p_{\ell_2}) = \frac{1}{(2\pi)^2} d\text{Lips}(s, p_{\chi_i}, p_{\chi_j}) ds_{\chi_i} d\text{Lips}(s_{\chi_i}, p_{\tilde{\ell}}, p_{\ell_1}) ds_{\tilde{\ell}} d\text{Lips}(s_{\tilde{\ell}}, p_{\chi_1}, p_{\ell_2}), \quad (\text{B.1})$$

$$d\text{Lips}(p_{\chi_i}, p_{\chi_j}) = \frac{q}{8\pi\sqrt{s}} \sin\theta \, d\theta, \quad (\text{B.2})$$

$$d\text{Lips}(s_{\chi_i}, p_{\tilde{\ell}}, p_{\ell_1}) = \frac{1}{2(2\pi)^2} \frac{|\vec{p}_{\ell_1}|^2}{m_{\chi_i}^2 - m_{\tilde{\ell}}^2} d\Omega_1, \quad (\text{B.3})$$

$$d\text{Lips}(s_{\tilde{\ell}}, p_{\chi_1}, p_{\ell_2}) = \frac{1}{2(2\pi)^2} \frac{|\vec{p}_{\ell_2}|^2}{m_{\tilde{\ell}}^2 - m_{\chi_1}^2} d\Omega_2, \quad (\text{B.4})$$

with $s_{\chi_i} = p_{\chi_i}^2$, $s_{\tilde{\ell}} = p_{\tilde{\ell}}^2$ and $d\Omega_i = \sin\theta_i \, d\theta_i \, d\phi_i$.

C Neutralino production and decay matrices

In this Section we give the analytical expressions for P, Σ_P^2 and D_1, D_2, Σ_{D1}^a in the center of mass system. Expressions for $\Sigma_P^{1,3}$ can be found in [5].

C.1 Neutralino production

The analytic expression P of Eq. (31) is independent of the neutralino polarization. It can be decomposed into contributions from the different production channels [5]:

$$P = P(ZZ) + P(Z\tilde{e}_R) + P(Z\tilde{e}_L) + P(\tilde{e}_R\tilde{e}_R) + P(\tilde{e}_L\tilde{e}_L), \quad (\text{C.1})$$

with

$$P(ZZ) = 2 \frac{g^4}{\cos^4\theta_W} |\Delta^s(Z)|^2 [(1 - P_-^3 P_+^3)(L_e^2 + R_e^2) - (P_-^3 - P_+^3)(L_e^2 - R_e^2)] E_b^2 \left\{ |O_{ij}^{''R}|^2 (E_{\chi_i} E_{\chi_j} + q^2 \cos^2\theta) - [(Re O_{ij}^{''R})^2 - (Im O_{ij}^{''R})^2] m_{\chi_i} m_{\chi_j} \right\}, \quad (\text{C.2})$$

$$P(Z\tilde{e}_R) = \frac{g^4}{\cos^2\theta_W} R_e (1 + P_-^3)(1 - P_+^3) E_b^2 Re \left\{ \Delta^s(Z) \left[-(\Delta^{t*}(\tilde{e}_R) f_{ei}^{R*} f_{ej}^R O_{ij}^{''R*} + \Delta^{u*}(\tilde{e}_R) f_{ei}^R f_{ej}^{R*} O_{ij}^{''R}) m_{\chi_i} m_{\chi_j} \right. \right. \\ \left. - (\Delta^{t*}(\tilde{e}_R) f_{ei}^{R*} f_{ej}^R O_{ij}^{''R} - \Delta^{u*}(\tilde{e}_R) f_{ei}^R f_{ej}^{R*} O_{ij}^{''R*}) 2E_b q \cos\theta \right. \\ \left. + (\Delta^{t*}(\tilde{e}_R) f_{ei}^{R*} f_{ej}^R O_{ij}^{''R} + \Delta^{u*}(\tilde{e}_R) f_{ei}^R f_{ej}^{R*} O_{ij}^{''R*}) (E_{\chi_i} E_{\chi_j} + q^2 \cos^2\theta) \right] \right\}, \quad (\text{C.3})$$

$$P(\tilde{e}_R\tilde{e}_R) = \frac{g^4}{4} (1 + P_-^3)(1 - P_+^3) E_b^2 \left\{ |f_{ei}^R|^2 |f_{ej}^R|^2 \left[(|\Delta^t(\tilde{e}_R)|^2 + |\Delta^u(\tilde{e}_R)|^2) (E_{\chi_i} E_{\chi_j} + q^2 \cos^2\theta) - (|\Delta^t(\tilde{e}_R)|^2 - |\Delta^u(\tilde{e}_R)|^2) 2E_b q \cos\theta \right] \right. \\ \left. - Re \{ (f_{ei}^{R*})^2 (f_{ej}^R)^2 \Delta^u(\tilde{e}_R) \Delta^{t*}(\tilde{e}_R) \} 2m_{\chi_i} m_{\chi_j} \right\}. \quad (\text{C.4})$$

To obtain the quantities $P(Z\tilde{e}_L), P(\tilde{e}_L\tilde{e}_L)$ one has to exchange in Eqs. (C.2) - (C.4)

$$\Delta^t(\tilde{e}_R) \rightarrow \Delta^t(\tilde{e}_L), \quad \Delta^u(\tilde{e}_R) \rightarrow \Delta^u(\tilde{e}_L), \quad P_-^3 \rightarrow P_+^3, \quad P_+^3 \rightarrow P_-^3 \\ R_e \rightarrow L_e, \quad O_{ij}^{''R} \rightarrow O_{ij}^{''L}, \quad f_{ei}^R \rightarrow f_{ei}^L, \quad f_{ej}^R \rightarrow f_{ej}^L. \quad (\text{C.5})$$

The propagators are defined as follows:

$$\Delta^s(Z) = \frac{i}{s - m_Z^2 + im_Z\Gamma_Z}, \quad \Delta^t(\tilde{e}_{R,L}) = \frac{i}{t - m_{\tilde{e}_{R,L}}^2}, \quad \Delta^u(\tilde{e}_{R,L}) = \frac{i}{u - m_{\tilde{e}_{R,L}}^2}, \quad (\text{C.6})$$

where m and Γ denote the mass and width of the exchanged particle, respectively, and $s = (p_{e^-} + p_{e^+})^2$, $t = (p_{e^-} - p_{\chi_j})^2$, and $u = (p_{e^-} - p_{\chi_i})^2$. The longitudinal beam polarization of $e^- (e^+)$ are denoted by $P_-^3 (P_+^3)$, respectively. Generally the contributions from the exchange of \tilde{e}_R (\tilde{e}_L) selectron exchange is enhanced and that of \tilde{e}_L (\tilde{e}_R) is suppressed for $P_-^3 > 0, P_+^3 < 0$ ($P_-^3 < 0, P_+^3 > 0$).

C.2 Neutralino polarization

The analytic expressions for the coefficient Σ_P^2 in Eq. (30) which describes the transversal polarization of neutralino $\tilde{\chi}_i^0$ perpendicular to the production plane decomposes into contributions from the different production channels [5]:

$$\Sigma_P^a(\tilde{\chi}_i^0) = \Sigma_P^a(\tilde{\chi}_i^0, ZZ) + \Sigma_P^a(\tilde{\chi}_i^0, Z\tilde{e}_R) + \Sigma_P^a(\tilde{\chi}_i^0, Z\tilde{e}_L) + \Sigma_P^a(\tilde{\chi}_i^0, \tilde{e}_R\tilde{e}_R) + \Sigma_P^a(\tilde{\chi}_i^0, \tilde{e}_L\tilde{e}_L). \quad (\text{C.7})$$

In the center of mass system they read [5]:

$$\begin{aligned} \Sigma_P^2(\tilde{\chi}_i^0, ZZ) &= -4\left(\frac{g^2}{\cos^2\theta_W}\right)^2 |\Delta^s(Z)|^2 [(1 - P_-^3 P_+^3)(L_e^2 - R_e^2) - (P_-^3 - P_+^3)(L_e^2 + R_e^2)] \\ &\quad \times m_{\chi_j} q E_b^2 \sin\theta \text{Re}(O_{ij}''^R) \text{Im}(O_{ij}''^R), \end{aligned} \quad (\text{C.8})$$

$$\begin{aligned} \Sigma_P^2(\tilde{\chi}_i^0, Z\tilde{e}_R) &= \frac{g^4}{\cos^2\theta_W} R_e (1 + P_-^3) (1 - P_+^3) m_{\chi_j} E_b^2 q \sin\theta \\ &\quad \times \text{Im}\left\{ \Delta^s(Z) [f_{ei}^R f_{ej}^{R*} O_{ij}''^R \Delta^{u*}(\tilde{e}_R) - f_{ei}^{R*} f_{ej}^R O_{ij}''^{R*} \Delta^{t*}(\tilde{e}_R)] \right\}, \end{aligned} \quad (\text{C.9})$$

$$\begin{aligned} \Sigma_P^2(\tilde{\chi}_i^0, \tilde{e}_R\tilde{e}_R) &= -\frac{g^4}{2} (1 + P_-^3) (1 - P_+^3) m_{\chi_j} E_b^2 q \sin\theta \\ &\quad \times \text{Im}\left\{ (f_{ei}^{R*})^2 (f_{ej}^R)^2 \Delta^u(\tilde{e}_R) \Delta^{t*}(\tilde{e}_R) \right\}. \end{aligned} \quad (\text{C.10})$$

To obtain the expressions for $\Sigma_P^2(\tilde{\chi}_i^0, Z\tilde{e}_L)$ and $\Sigma_P^2(\tilde{\chi}_i^0, \tilde{e}_L\tilde{e}_L)$ one has to apply the exchanges (C.5) in Eq. (C.8) - (C.10).

C.3 Neutralino decay matrix

The neutralino decay matrix is given by Eq. (31):

$$\rho_{D1}(\tilde{\chi}_i^0)_{\lambda'_i \lambda_i} = \delta_{\lambda'_i \lambda_i} D_1 + \sum_a \sigma_{\lambda'_i \lambda_i}^a \Sigma_{D1}^a.$$

The expansion coefficients D_1 and Σ_{D1}^a for the decay into the right slepton are ($\ell = e, \mu$):

$$D_1 = \frac{g^2}{2} |f_{\ell i}^R|^2 (m_{\chi_i}^2 - m_{\ell}^2), \quad (\text{C.11})$$

$$\Sigma_{D1}^a = g^2 |f_{\ell i}^R|^2 m_{\chi_i} (s_{\chi_i}^a \cdot p_{\ell_1}), \quad (\text{C.12})$$

respectively, with $s_{\chi_i}^a$ the neutralino spinvector and p_{ℓ_1} the lepton ℓ_1 momentum vector. For the decay into the left selectron or smuon they are:

$$D_1 = \frac{g^2}{2} |f_{\ell i}^L|^2 (m_{\chi_i}^2 - m_{\tilde{\ell}}^2), \quad (\text{C.13})$$

$$\Sigma_{D1}^a = -g^2 |f_{\ell i}^L|^2 m_{\chi_i} (s_{\chi_i}^a \cdot p_{\ell_1}). \quad (\text{C.14})$$

For the decay into the stau $\tilde{\tau}_k$ ($k = 1, 2$) they read:

$$D_1 = \frac{g^2}{2} (|a_{ki}^{\tilde{\tau}}|^2 + |b_{ki}^{\tilde{\tau}}|^2) (m_{\chi_i}^2 - m_{\tilde{\tau}_k}^2), \quad (\text{C.15})$$

$$\Sigma_{D1}^a = g^2 (|a_{ki}^{\tilde{\tau}}|^2 - |b_{ki}^{\tilde{\tau}}|^2) m_{\chi_i} (s_{\chi_i}^a \cdot p_{\ell_1}). \quad (\text{C.16})$$

The decay of the right (R) or left (L) slepton into lepton and $\tilde{\chi}_1^0$ is given by ($\ell = e, \mu$):

$$D_2 = g^2 |f_{\ell 1}^{R,L}|^2 (m_{\tilde{\ell}}^2 - m_{\chi_1}^2), \quad (\text{C.17})$$

and into staus $\tilde{\tau}_k$ by:

$$D_2 = g^2 (|a_{k1}^{\tilde{\tau}}|^2 + |b_{k1}^{\tilde{\tau}}|^2) (m_{\tilde{\tau}_k}^2 - m_{\chi_1}^2). \quad (\text{C.18})$$

References

- [1] H. E. Haber and G. L. Kane, Phys. Rep. **117** (1985) 75.
- [2] TESLA Technical Design Report, Part III, *Physics at an e^+e^- Linear Collider*, eds. R.-D. Heuer, D. Miller, F. Richard and P. Zerwas, [arXiv:hep-ph/0106315].
- [3] S. Y. Choi, H. S. Song and W. Y. Song, Phys. Rev. **D 61** (2000) 075004.
- [4] S. Y. Choi, J. Kalinowski, G. Moortgat-Pick and P. M. Zerwas, Eur. Phys. J. **C 22** (2001) 563; Addendum-ibid. **C 23** (2001) 769; S. Y. Choi [arXiv:hep-ph/0308060].
- [5] G. Moortgat-Pick, H. Fraas, A. Bartl and W. Majerotto, Eur. Phys. J. **C 9** (1999) 521; Erratum-ibid. **C 9** (1999) 549.
- [6] J. F. Donoghue, Phys. Rev. **D 18** (1978) 1632.
- [7] Y. Kizukuri and N. Oshimo, Phys. Lett. **B 249** (1990) 449.
- [8] G. Valencia, [arch-ive/9411441].
- [9] A. Bartl, H. Fraas, T. Kernreiter and O. Kittel, [arXiv:hep-ph/0306304].
- [10] H. E. Haber, *Proceedings of the 21st SLAC Summer Institute on Particle Physics*, eds. L. DeProcel, Ch. Dunwoodie, Stanford 1993, 231.
- [11] A. Bartl, K. Hidaka, T. Kernreiter and W. Porod, Phys. Rev. **D 66**, 115009 (2002) [arXiv:hep-ph/0207186].

- [12] L. J. Hall and J. Polchinski, Phys. Lett. **B 152** (1989) 335.
- [13] S. T. Petcov, Phys. Lett. **B 139** (1984) 421; G. Moortgat-Pick and H. Fraas, Eur. Phys. J. **C 25** (2002) 189.
- [14] I. S. Altarev et al., Phys. Lett. **B 276** (1992) 242; I. S. Altarev et al., Phys. Atom. Nucl. **59** (1996) 1152 and Yad. Fiz. **59 N 7**; E. D. Commins, S. B. Ross, D. DeMille, B. C. Regan, Phys. Rev. **A 50** (1994) 2960.
- [15] P. Nath, talk at the 9th International Conference on Supersymmetry and Unification of Fundamental Interactions, 11-17 June 2001, Dubna (hep-ph/0107325) and references therein.

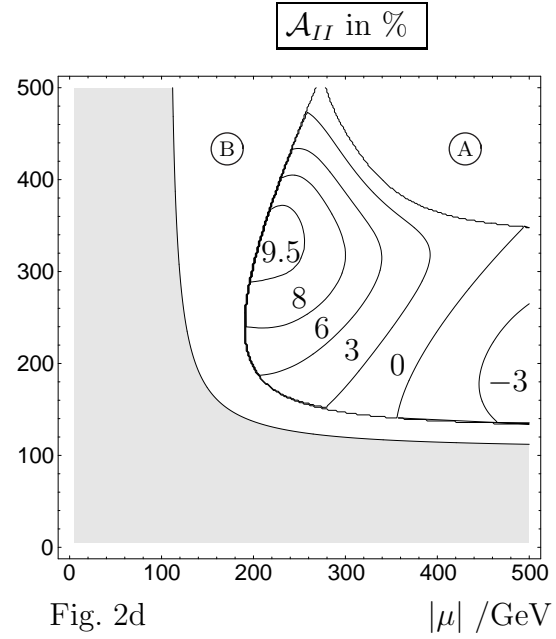
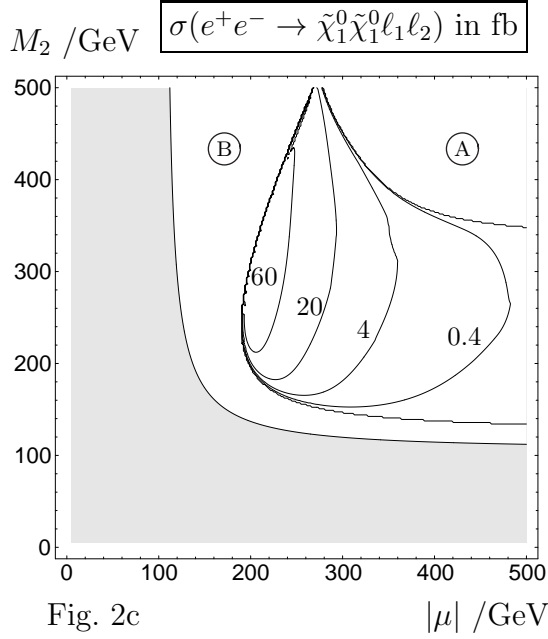
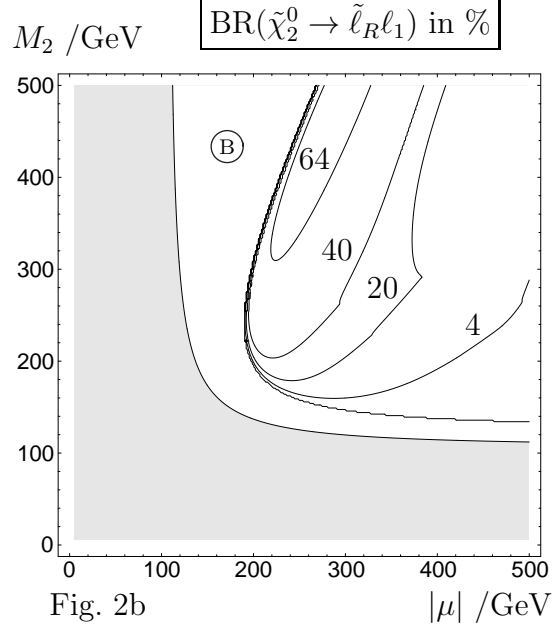
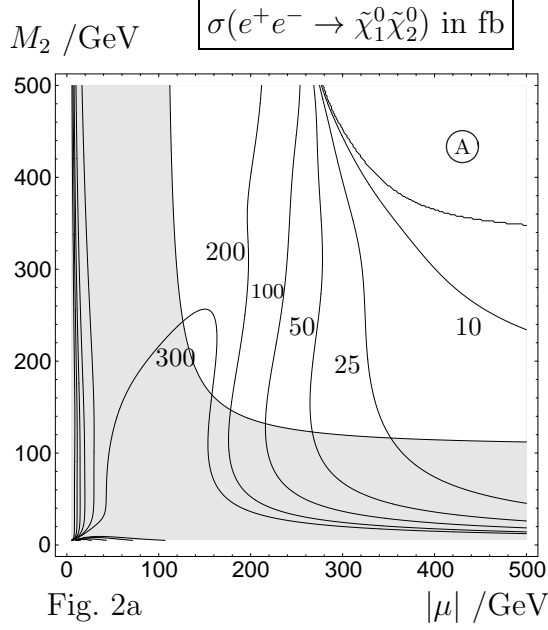


Figure 2: Contour plots for 2a: $\sigma(e^+e^- \rightarrow \tilde{\chi}_1^0 \tilde{\chi}_2^0)$, 2b: $\text{BR}(\tilde{\chi}_2^0 \rightarrow \tilde{\ell}_R \ell_1)$, $\ell = e, \mu$, 2c: $\sigma(e^+e^- \rightarrow \tilde{\chi}_1^0 \tilde{\chi}_2^0) \times \text{BR}(\tilde{\chi}_2^0 \rightarrow \tilde{\ell}_R \ell_1) \times \text{BR}(\tilde{\ell}_R \rightarrow \tilde{\chi}_1^0 \ell_2)$ with $\text{BR}(\tilde{\ell}_R \rightarrow \tilde{\chi}_1^0 \ell_2) = 1$, 2d: the asymmetry \mathcal{A}_{II} , in the $|\mu|$ - M_2 plane for $\varphi_{M_1} = 0.5\pi$, $\varphi_\mu = 0$, taking $\tan\beta = 10$, $m_0 = 100$ GeV, $A_\tau = -250$ GeV, $\sqrt{s} = 500$ GeV, $P_- = 0.8$ and $P_+ = -0.6$. The area A (B) is kinematically forbidden by $m_{\tilde{\chi}_1^0} + m_{\tilde{\chi}_2^0} > \sqrt{s}$ ($m_{\tilde{\ell}_R} > m_{\tilde{\chi}_2^0}$). The gray area is excluded by $m_{\tilde{\chi}_1^\pm} < 104$ GeV.

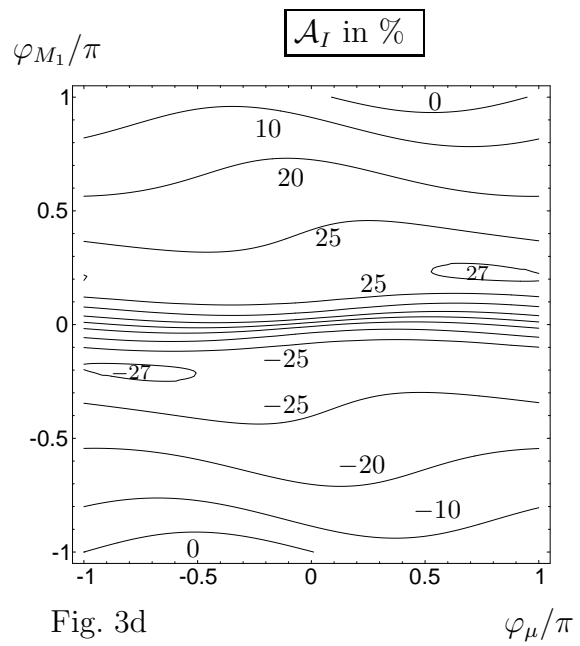
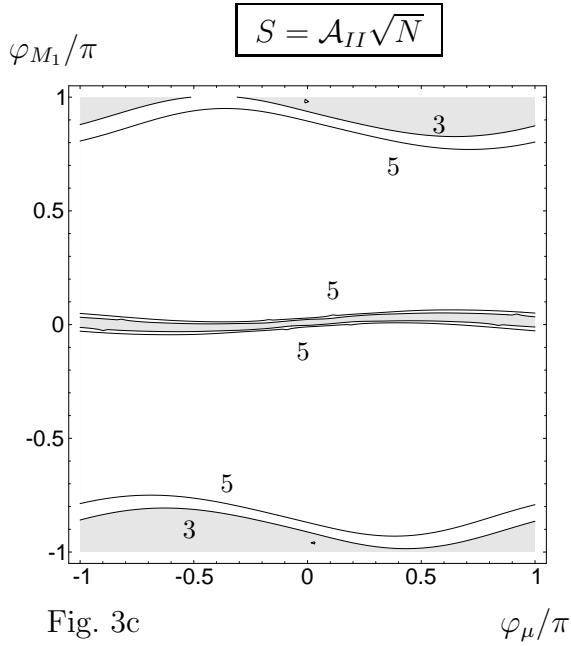
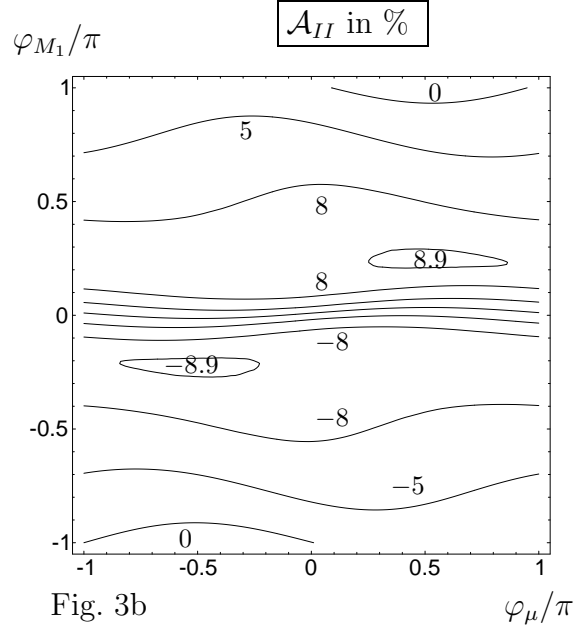
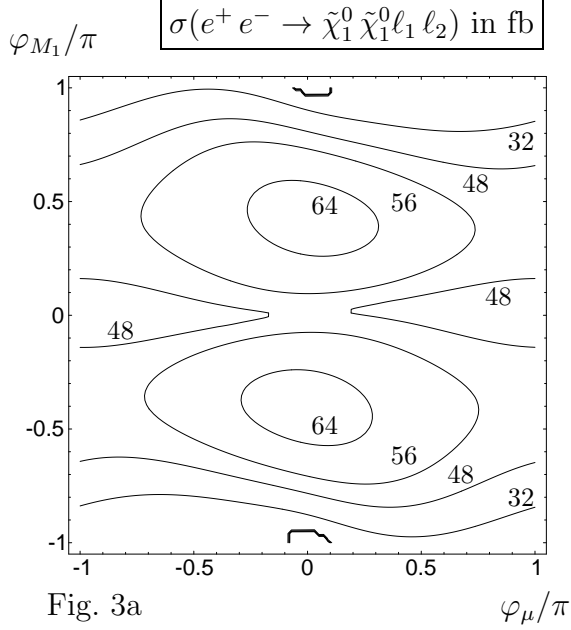


Figure 3: Contour plots for 3a: $\sigma(e^+e^- \rightarrow \tilde{\chi}_1^0 \tilde{\chi}_2^0) \times \text{BR}(\tilde{\chi}_2^0 \rightarrow \tilde{\ell}_R \ell_1) \times \text{BR}(\tilde{\ell}_R \rightarrow \tilde{\chi}_1^0 \ell_2)$ with $\text{BR}(\tilde{\ell}_R \rightarrow \tilde{\chi}_1^0 \ell_2) = 1$, 3b: the asymmetry \mathcal{A}_{II} , 3c: the standard deviation S , 3d: the asymmetry \mathcal{A}_I , in the φ_μ - φ_{M_1} plane for $M_2 = 400$ GeV and $|\mu| = 240$ GeV, taking $\tan\beta = 10$, $m_0 = 100$ GeV, $A_\tau = -250$ GeV, $\sqrt{s} = 500$ GeV, $P_- = 0.8$ and $P_+ = -0.6$. For $\varphi_{M_1}, \varphi_\mu = 0$ we have $m_{\tilde{\ell}_R} = 221$ GeV, $m_{\tilde{\chi}_1^0} = 178$ GeV and $m_{\tilde{\chi}_2^0} = 243$ GeV.

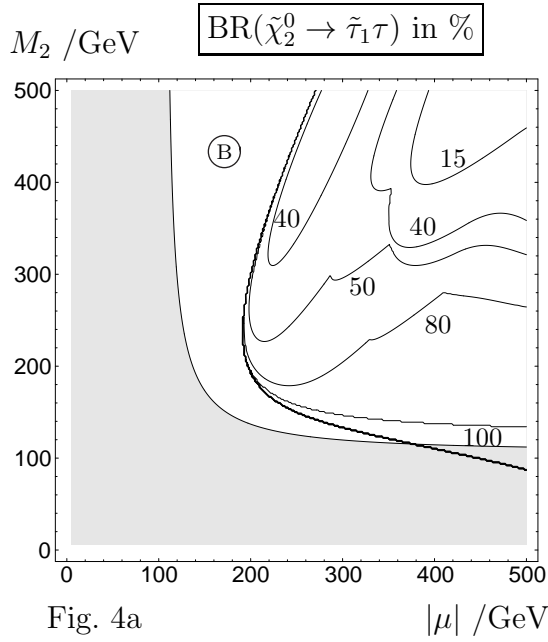


Fig. 4a

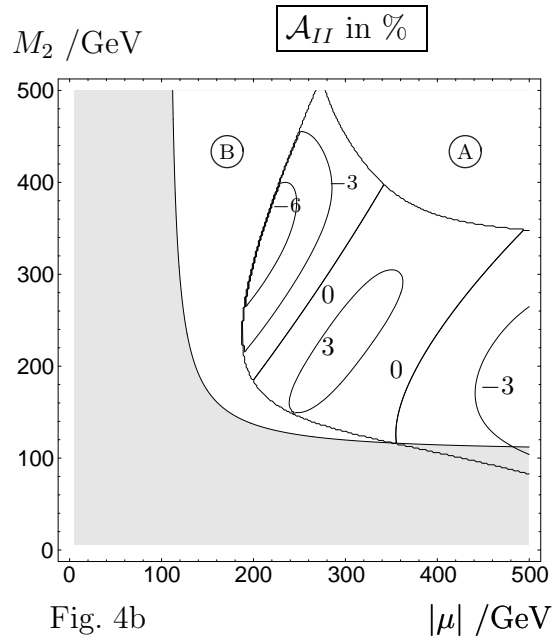


Fig. 4b

Figure 4: Contour plots for 4a: $\text{BR}(\tilde{\chi}_2^0 \rightarrow \tilde{\tau}_1 \tau)$ and 4b: the asymmetry \mathcal{A}_{II} , in the $|\mu|$ - M_2 plane for $\varphi_{M_1} = 0.5\pi$, $\varphi_\mu = 0$ and $A_\tau = -250$ GeV, taking $\tan \beta = 10$, $m_0 = 100$ GeV, $\sqrt{s} = 500$ GeV, $P_- = 0.8$ and $P_- = -0.6$. The area A (B) is kinematically forbidden by $m_{\tilde{\chi}_1^0} + m_{\tilde{\chi}_2^0} > \sqrt{s}$ ($m_{\tilde{\tau}_1} > m_{\tilde{\chi}_2^0}$). The gray area is excluded by $m_{\tilde{\chi}_1^\pm} < 104$ GeV.

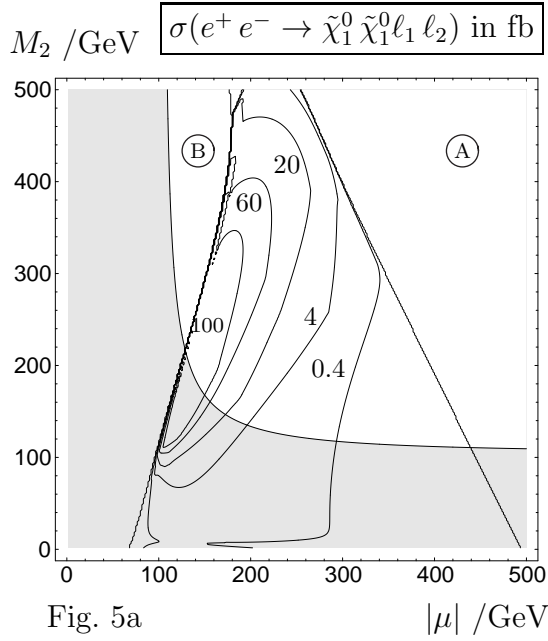


Fig. 5a

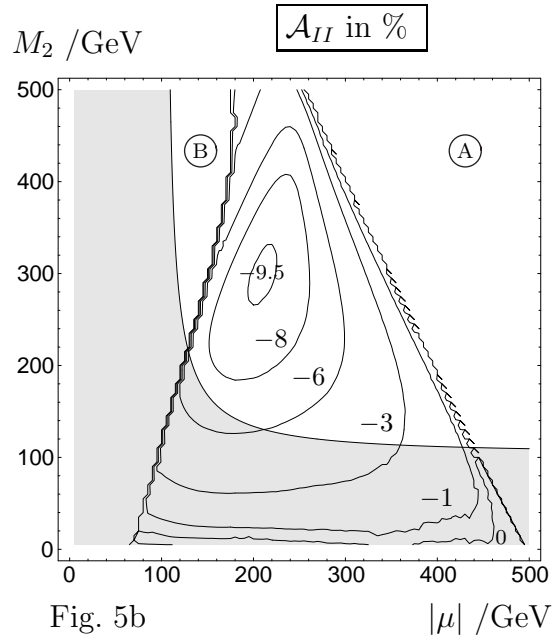


Fig. 5b

Figure 5: Contour plots for 5a: $\sigma(e^+e^- \rightarrow \tilde{\chi}_1^0 \tilde{\chi}_3^0) \times \text{BR}(\tilde{\chi}_3^0 \rightarrow \tilde{\ell}_R \ell_1) \times \text{BR}(\tilde{\ell}_R \rightarrow \tilde{\chi}_1^0 \ell_2)$ with $\text{BR}(\tilde{\ell}_R \rightarrow \tilde{\chi}_1^0 \ell_2) = 1$ and $\ell = e, \mu$, 5b: the asymmetry \mathcal{A}_{II} , in the $|\mu|$ - M_2 plane for $\varphi_{M_1} = 0.5\pi$, $\varphi_\mu = 0$, taking $\tan\beta = 10$, $m_0 = 100$ GeV, $A_\tau = -250$ GeV, $\sqrt{s} = 500$ GeV, $P_- = 0.8$ and $P_+ = -0.6$. The area A (B) is kinematically forbidden by $m_{\tilde{\chi}_1^0} + m_{\tilde{\chi}_3^0} > \sqrt{s}$ ($m_{\tilde{\ell}_R} > m_{\tilde{\chi}_3^0}$). The gray area is excluded by $m_{\tilde{\chi}_1^\pm} < 104$ GeV.

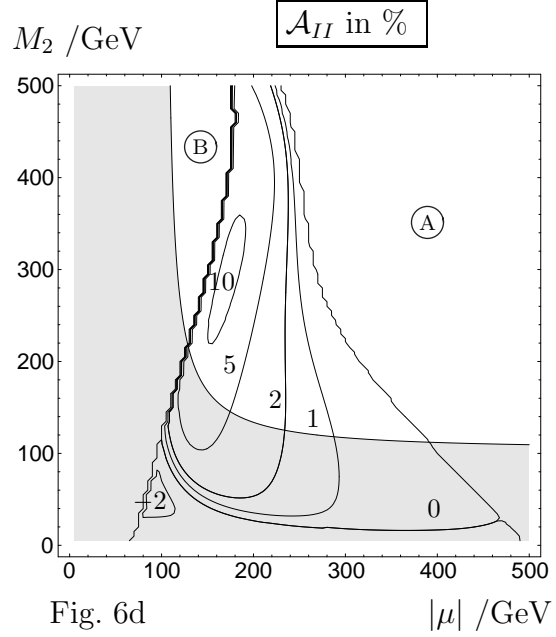
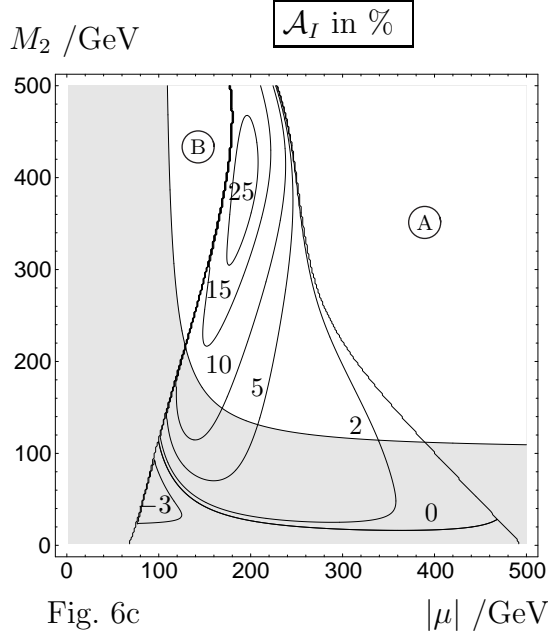
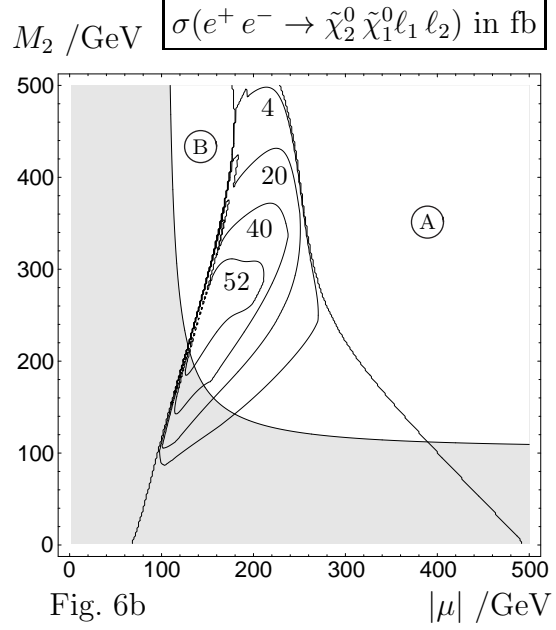
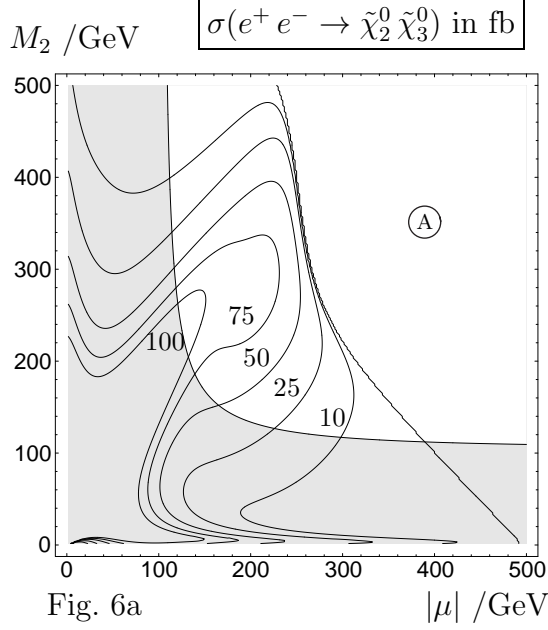


Figure 6: Contour plots for 6a: $\sigma(e^+e^- \rightarrow \tilde{\chi}_2^0 \tilde{\chi}_3^0)$, 6b: $\sigma(e^+e^- \rightarrow \tilde{\chi}_2^0 \tilde{\chi}_3^0) \times \text{BR}(\tilde{\chi}_3^0 \rightarrow \tilde{\ell}_R \ell_1) \times \text{BR}(\tilde{\ell}_R \rightarrow \tilde{\chi}_1^0 \ell_2)$ for $\ell = e, \mu$, and $\text{BR}(\tilde{\ell}_R \rightarrow \tilde{\chi}_1^0 \ell_2) = 1$, 6c: the asymmetry \mathcal{A}_I , 6d: the asymmetry \mathcal{A}_{II} , in the $|\mu|$ - M_2 plane for $\varphi_{M_1} = 0.5\pi$, $\varphi_\mu = 0$, taking $\tan\beta = 10$, $m_0 = 100$ GeV, $A_\tau = -250$ GeV, $\sqrt{s} = 500$ GeV, $P_- = 0.8$ and $P_+ = -0.6$. The area A (B) is kinematically forbidden by $m_{\tilde{\chi}_2^0} + m_{\tilde{\chi}_3^0} > \sqrt{s}$ ($m_{\tilde{\ell}_R} > m_{\tilde{\chi}_3^0}$). The gray area is excluded by $m_{\tilde{\chi}_1^\pm} < 104$ GeV.

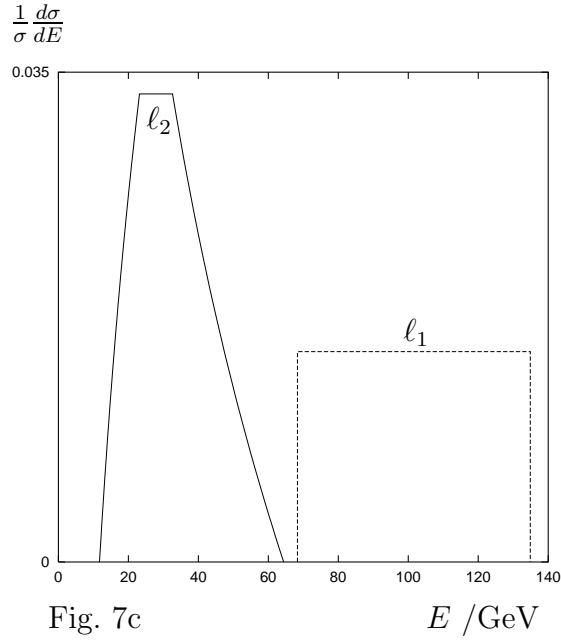
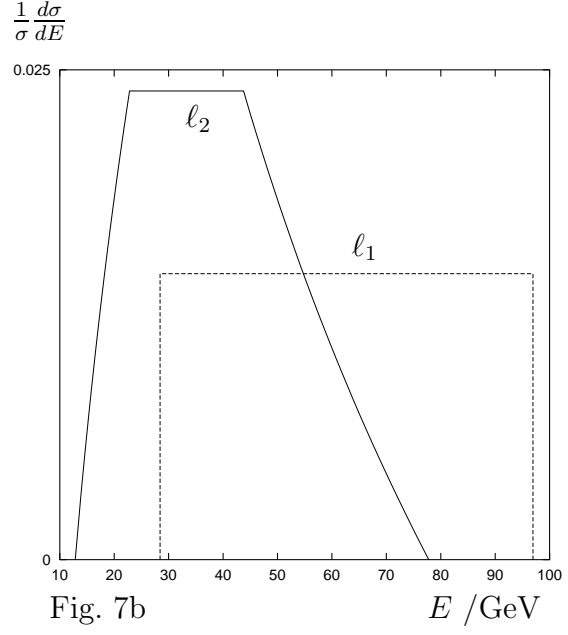
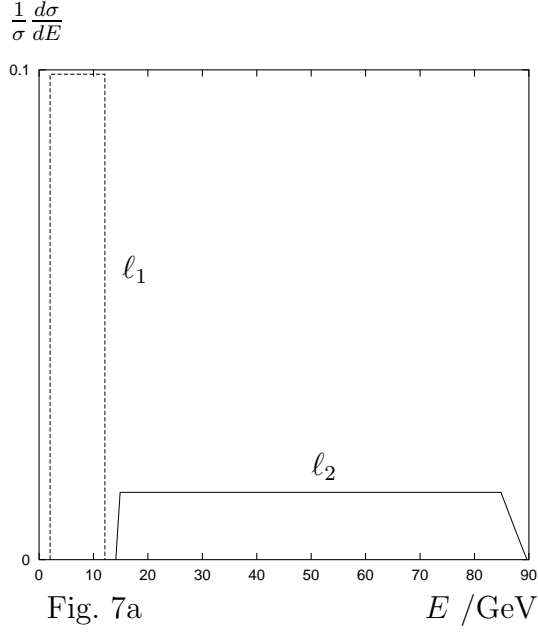


Figure 7: Possible types of energy distributions in the laboratory system for ℓ_1 (dashed line) and ℓ_2 (solid line) for $e^+e^- \rightarrow \tilde{\chi}_1^0 \tilde{\chi}_2^0$ and the subsequent decays $\tilde{\chi}_2^0 \rightarrow \tilde{\ell}_R \ell_1$ and $\tilde{\ell}_R \rightarrow \tilde{\chi}_1^0 \ell_2$, for $M_2 = 300$ GeV, $m_{\tilde{\ell}_R} = 180$ GeV, $\tan \beta = 10$ and $\{|\mu|, m_{\chi_1}, m_{\chi_2}\}/\text{GeV} = \{200, 140, 185\}$, $\{300, 145, 240\}$, $\{500, 150, 300\}$ in a, b, c respectively.